Carbohydrate Polymers 83 (2011) 1565–1569

Contents lists available at ScienceDirect

Carbohydrate Polymers

journal homepage: www.elsevier.com/locate/carbpol

Preparation of chitosan–zinc oxide complex during chitin deacetylation

Shanmugam Anandhavelu, Sivalingam Thambidurai*

Department of Industrial Chemistry, School of Chemistry, Alagappa University, Karaikudi 630003, Tamil Nadu, India

ARTICLE INFO

Article history:
Received 22 September 2010
Received in revised form 5 October 2010
Accepted 6 October 2010
Available online 12 October 2010

Keywords:
Zinc chloride
Rod-like complex
Chitosan
UV absorption

ABSTRACT

Novel chitosan–ZnO complexes are prepared using zinc chloride, sodium hydroxide and chitin as source materials by direct precipitation method. Four chitosan–ZnO complexes are prepared for different concentrations of source material. The chitosan–ZnO complex formations have been confirmed by FTIR spectroscopic analysis. Hexagonal structure and crystalline size (35–51 nm) of zinc oxide are determined by XRD. Rod-like particle shape of chitosan–ZnO complex from SEM images, higher UV rays absorption in the region of 200–275 nm by UV–vis and higher UV emission at 422 nm by photoluminescence spectrophotometer are recorded. The rod-like chitosan–zinc oxide was obtained with optimum concentration of 45% NaOH and 15% $ZnCl_2$. The size of the complex was increased with increase of sodium hydroxide concentration.

1. Introduction

With advent of nanotechnology, semiconductor nanoparticles has attracted much attention due to their novel optical, electrical and mechanical properties. Among various semiconductor nanoparticles, nanosized zinc oxide (ZnO) particles are the most frequently studied because of their interest in fundamental study and also their applied aspects such as in solar energy conversion, varistors, luminescence, photo-catalysis, electrostatic dissipative coating, transparent UV protection films and chemical sensors. Previously, ZnO nanoparticles have been prepared by techniques including the sol–gel method (Hubbard, Culpepper, & Howell, 2006; Lee, Yeo, & Jeong, 2003), precipitation (Wang & Muhammed, 1999), hydrothermal synthesis (Xu et al., 2004) and spray pyrolysis (Tani, Mädler, & Pratsinis, 2002).

Zhu and Zhou (2008) synthesized pure ZnO nanoparticles by solid-state reaction with a 1:4 molar ratio of $ZnSO_4{\cdot}7H_2O$ to NaOH at room temperature. By introducing changes into the procedure of its chemical synthesis, the microstructural and physical properties of ZnO can be modified. Recently, hybrid materials based on chitosan have been developed, including conducting polymers, metal nanoparticles and oxide agents, due to excellent properties of individual components and outstanding synergistic effects simultaneously (Son, Yeom, Song, Lee, & Hwang, 2009; Zhang, Su, Zhao, & Tan, 2008). Since, chitosan has tremendous ability to form metal complexes with zinc metal (Muzzarelli, 1973; Muzzarelli & Sipos, 1971; Muzzarelli & Tubertini, 1969) because of its amine groups and hydroxyl groups currently, chitosan–ZnO complex attracted great interests for its potential use as UV protector and medicament.

By controlling the amount of Zn salt in the preparation method, high antibacterial activities of ZnO nanoparticles were successfully prepared via a new method of sol-cast transformation which makes it a homogeneous dispersion within chitosan matrix (Li, Deng, Deng, Liu, & Xin, 2010; Xu et al., 2004). In the present investigation, a new method of precipitation was followed to prepare chitosan–ZnO complex by addition of $ZnCl_2$ during chitin deacetylation process.

2. Experimental details

2.1. Materials

Analytical grade of zinc chloride (95%), sodium hydroxide (98%) and acetic acid (99.7%) was purchased from Fischer Chemic Ltd., Chennai, India. The shells of crab were scraped free of loose tissue, washed, dried and grounded to pass through a 250 μm sieve, then subjected to demineralization and deproteinization (Al-Sagheer, Al-Sughayer, Muslim, & Elsabee, 2009). Double distilled water was used throughout the experiment.

2.2. Deacetylation

Two methods were used to prepare chitosan from chitin. First, the extracted chitin was treated with NaOH 45% (w/v) (1 part of chitin and 60 parts of NaOH) at 70 °C for 2 h and the formed chitosan samples were purified by dissolving in 2% acetic acid. The supernatant solution was discarded, and the remaining formed precipitate was allowed to settle for 24 h by adding 200 parts of distilled water. The clear solution was removed and then remain-

---

* Corresponding author. Tel.: +91 4565 228836; fax: +91 4565 228836.
E-mail address: sthambi01@yahoo.co.in (S. Thambidurai).

0144-8617/$ – see front matter © 2010 Elsevier Ltd. All rights reserved.
doi:10.1016/j.carbpol.2010.10.006

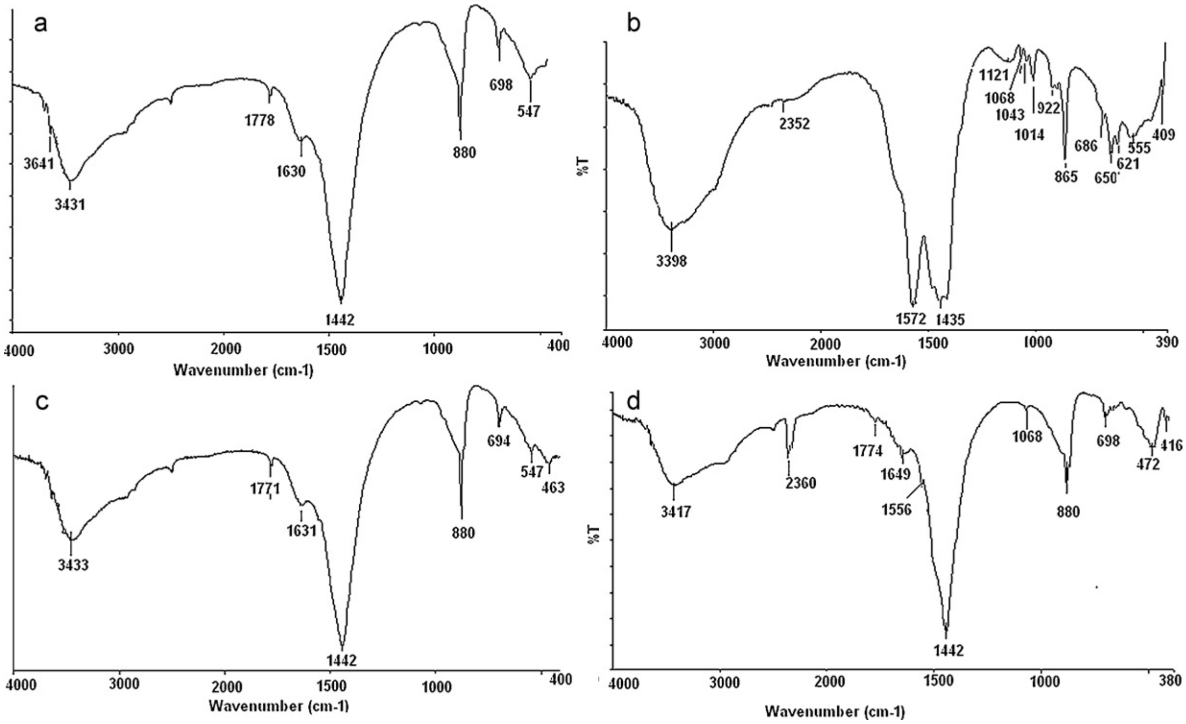

Fig. 1. FTIR spectra of chitosan and its complexes: (a) control, (b) N30, (c) N45 and (d) N60.

ing suspension filtered using suction pump and dried in the oven at 110 °C for 1 h. This sample was taken as control sample. In the second method, the extracted chitin was treated with a mixture of $ZnCl_2$ and NaOH having three proportions of (15%, 30%), (15%, 45%) and (15%, 60%) and these samples were designated as N30, N45 and N60 respectively. All the samples were then washed and dried as stated above.

2.3. Instrumental analyses

The functional group identification was done using FTIR spectroscopy (Thermo-Nicolet-380 Madison, USA model) in the spectral range of 4000–400 cm^{-1}. The structural morphology of the prepared samples was carried out using X-ray diffractometer (X'Pert PRO diffractometer) of Cu Kα radiation ($\lambda = 0.15406$ nm) with the scanning rate of 0.01°/step with 2θ ranging from 10° to 80°. The SEM images of the chitosan were depicted using scanning electron microscope (Hitachi S3000 H SEM). The absorption and emission spectra were recorded using UV–visible spectrophotometer (2401 PC model; Shimadzu, Kyoto, Japan) in the wavelength range of 200–800 nm and photoluminescence (Cary Eclipse fluorescence spectrophotometer).

3. Results and discussion

3.1. FTIR spectroscopy

The FTIR spectrum of chitosan and its complex are shown in Fig. 1. The characteristic peak at 3431 cm^{-1}, corresponding to the stretching vibration of $-NH_2$ group and –OH group (Fig. 1a) were shifted to lower frequency (3398 and 3417 cm^{-1}), with addition of $ZnCl_2$ (Fig. 1b–d). Appearance of band at 1630 cm^{-1} assigned to the bending vibration of $-NH_2$ group present in the control sample (Qin, Xiao, Du, Shi, & Chen, 2002) was shifted to a lower wave number (1572 cm^{-1}) for N30 sample and a higher wave number (1649 cm^{-1}) for N60 sample. This indicates that the $-NH_2$ group and –OH group were involved in complexation (Tang, Huang, & Lim, 2003; Tang & Hon, 2000). The C=O band formation of chitosan has been confirmed by the vibrational peak at 1778–1771 cm^{-1} in Fig. 1a and do not appear in Fig. 1b. This suggests that a monomolecular layer on nanosized ZnO surface be formed (Hong, Pan, Qian, & Li, 2006). The presence of the peak at 1442 cm^{-1} in the complex was assigned to the $-CH_2$ scissoring vibrational mode and vibrational peaks at 880 and 865 cm^{-1} was assigned to glucopyranose ring of chitosan. The –N–H wagging mode of chitosan has been confirmed by the peaks at 698 cm^{-1} which is shifted to 694, 686 cm^{-1}. In addi-

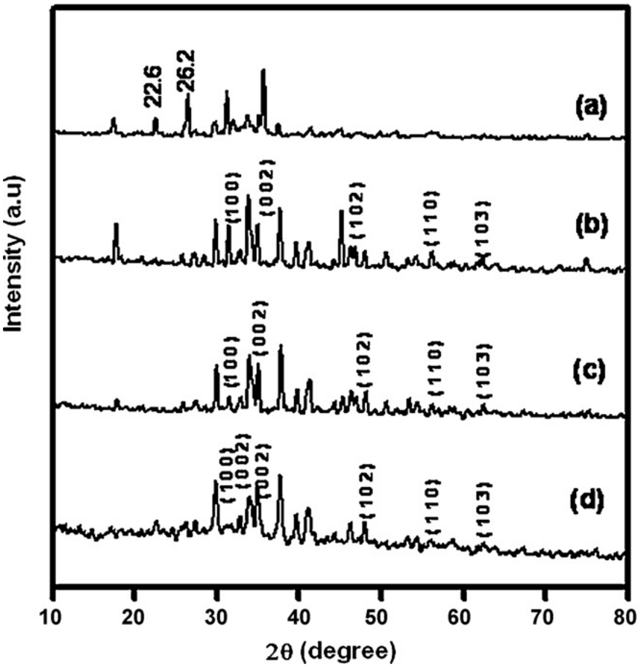

Fig. 2. XRD patterns of chitosan and its complexes: (a) control, (b) N30, (c) N45 and (d) N60.

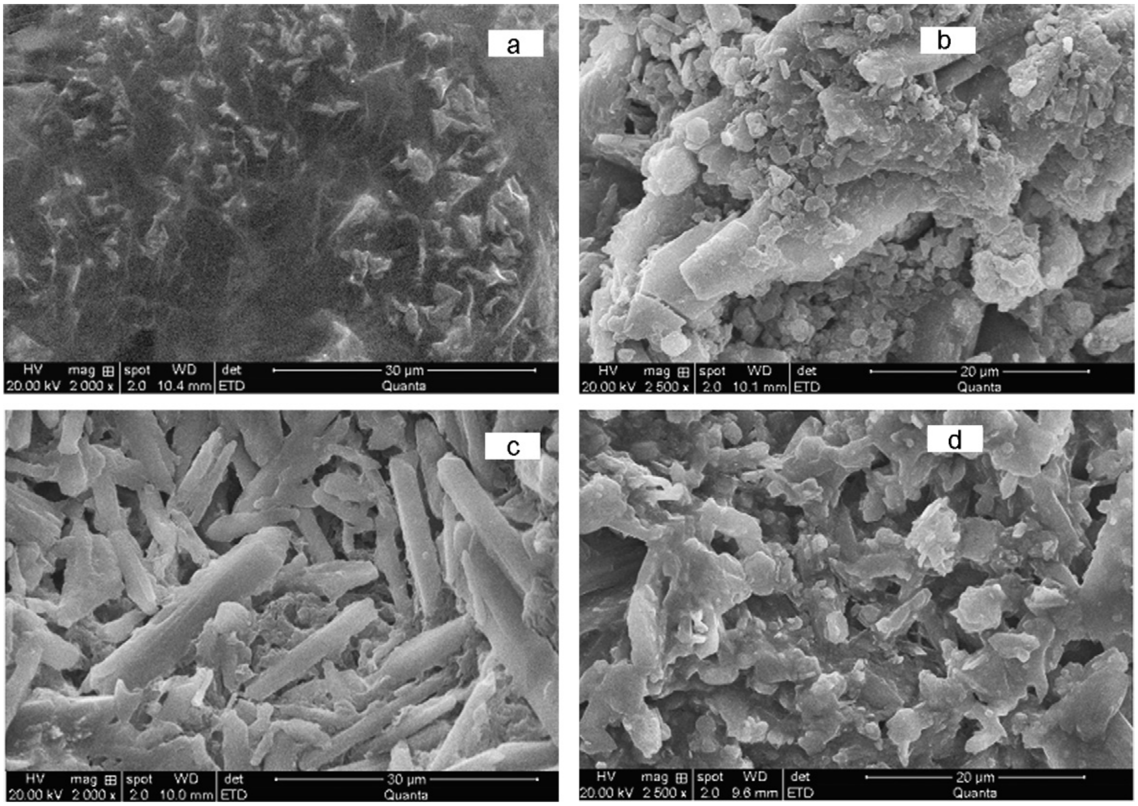

Fig. 3. SEM image of chitosan and its complexes: (a) control, (b) N30, (c) N45 and (d) N60.

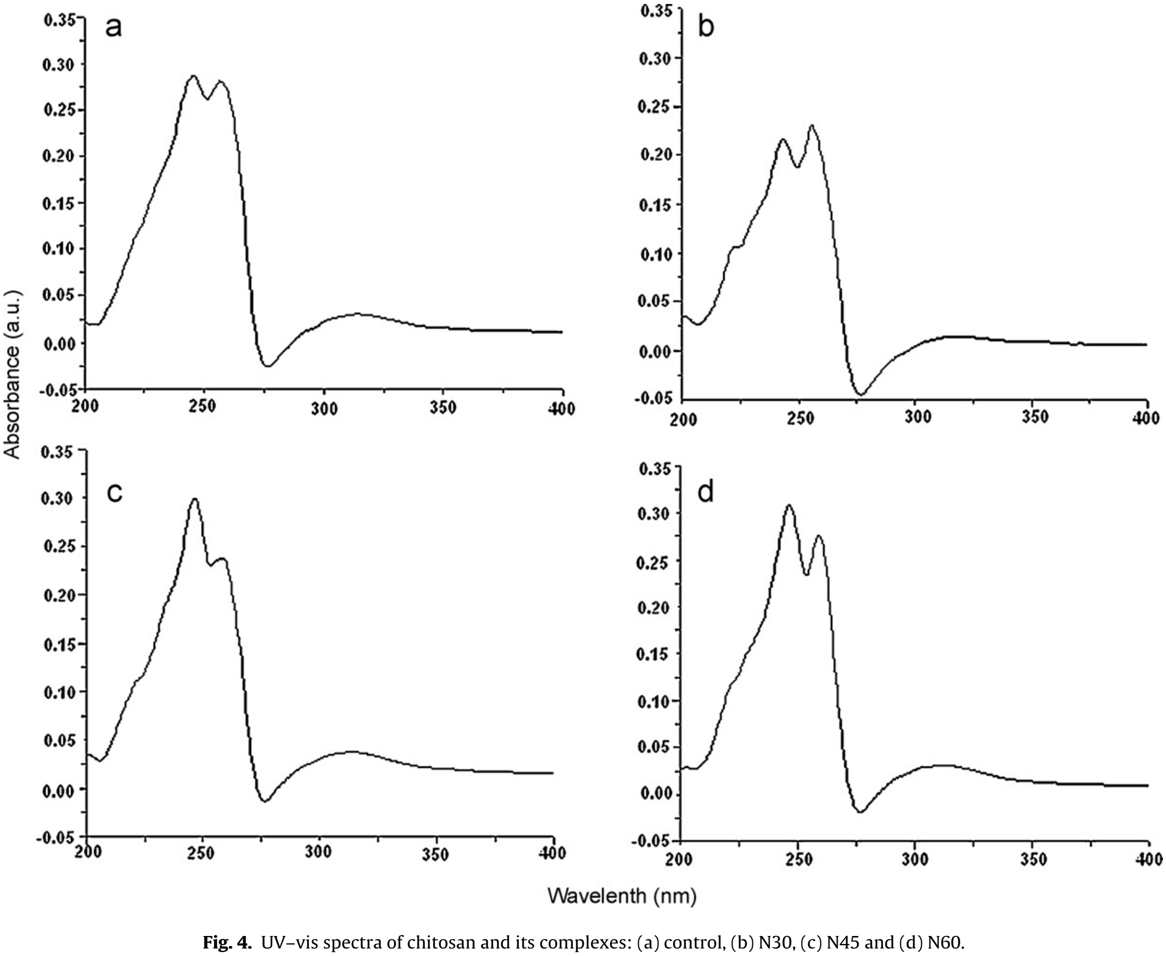

Fig. 4. UV–vis spectra of chitosan and its complexes: (a) control, (b) N30, (c) N45 and (d) N60.

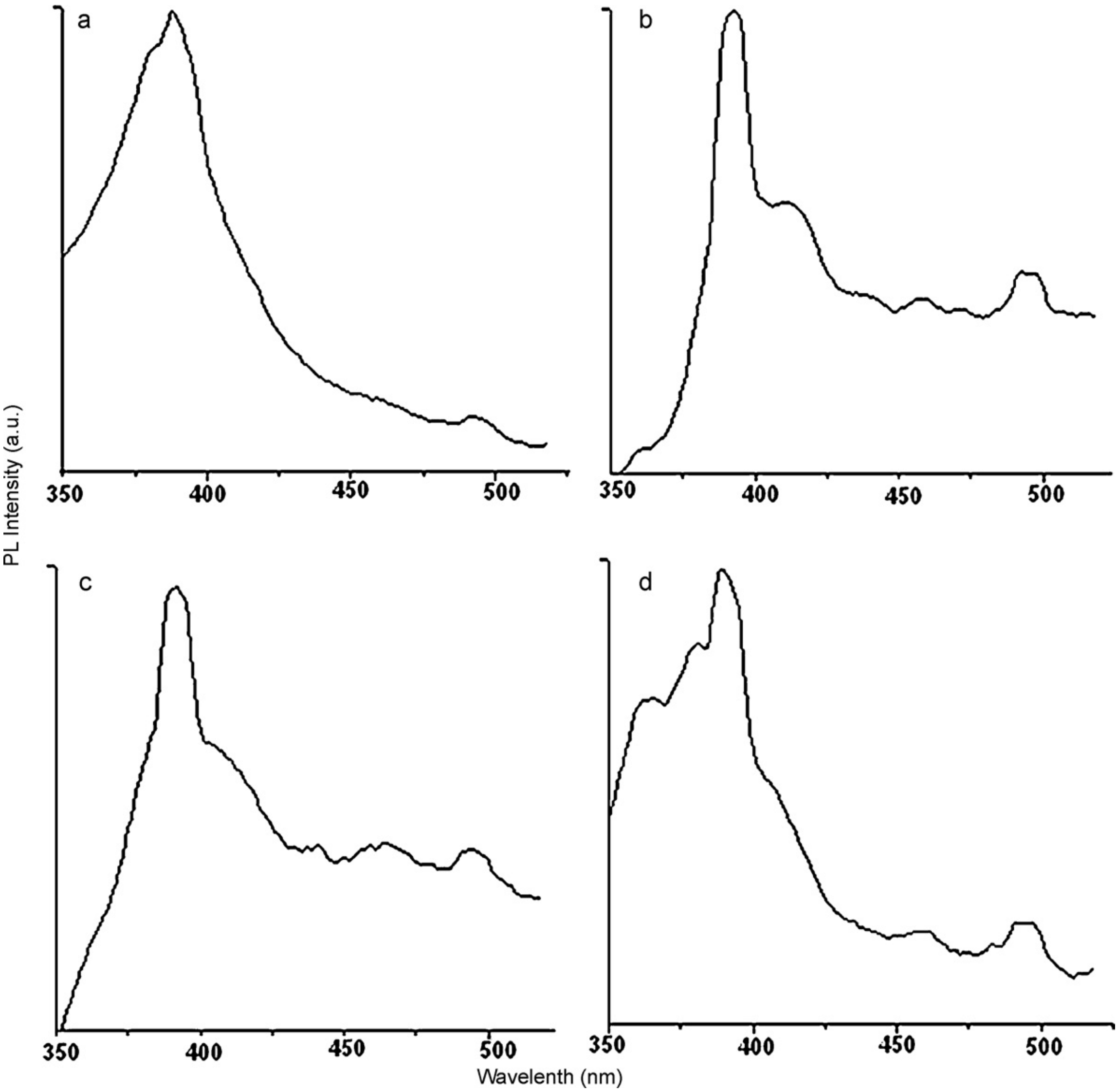

Fig. 5. PL spectra of chitosan and its complexes: (a) control, (b) N30, (c) N45 and (d) N60.

tion to that, the presence of some new peaks at 409, 463, 472 and 416 cm^{-1} in the chitosan–Zn complex confirmed the chitosan–ZnO complex formation (Li et al., 2010; Xu et al., 2004).

3.2. XRD spectrometry

Semicrystalline nature of the control sample (Fig. 2a) was confirmed by the appearance of characteristic peaks at $2\theta = 22.6^\circ$, 26.2° (Li, Zhou, & Zhang, 2009; Tang, Huang, & Lim, 2003). The peaks at $2\theta = 31.7^\circ$, 34.3°, 47.4°, 56.5°, 62.7°, 66.3°, 67.8° of complex as shown in Fig. 2b–d are corresponding to (1 0 0), (1 1 0), (1 0 3), (1 1 2) (1 0 2), (1 0 3), (2 0 0) and (0 0 2) lattice plane of zinc oxide (JCPDS No. 36-1451). Hexagonal structure of ZnO was confirmed by the crystalline peaks and particle size calculated using Dye–Scherer ($D = .94\lambda/\beta\cos\theta$) equation varies from 35 to 51 nm which mainly depends on the sodium hydroxide concentration. Moreover, the presence of ZnO particles impeded the order of polymer chains by both steric effect and intermolecular hydrogen bonds (Li et al., 2010).

3.3. Scanning electron microscopy

Surface images of synthesized chitosan and its complex with (×2500) magnification are shown in Fig. 3a–d. Surface image of the control sample shows smooth as well as particle agglomerations (Fig. 3a). The denser area of the image may be due to the formation of by-products. The sharp characteristic peaks observed in the XRD pattern may be due to the presence of crystallites, which is very close in agreement with this SEM results. N30 sample shows a denser and highly rough surface. It also shows some hexagonal structure crystallites with size of 100–200 nm which belongs to ZnO particles (Fig. 3b). When the concentration of sodium hydroxide increases from 30% to 45%, a rod-like formation of ZnO was observed (Fig. 3c) and disappeared with further increase of sodium hydroxide from 45% to 60% (Fig. 3d). Increasing the sodium hydroxide concentration appreciably increase the interaction between chitin and zinc chloride.

3.4. UV–visible spectroscopy

The solar UV radiation is actually composed of UV-A (400–315 nm), UV-B (315–290 nm) and UV-C (290–200 nm). UV spectra (200–400 nm) of control, N30, N45 and N60 samples are shown in Fig. 4a–d. It was noted from the spectra, that N45 and N60 samples show higher absorption, whereas N30 sample shows lower absorption in the UV region of 200–275 nm than control sample. The same trend was also noticed in the region of 290–315 nm.

The increase in absorption in the UV spectra may be due to the formation of chitosan–ZnO complex (Li et al., 2010).

3.5. Photoluminescence spectral studies

Fig. 5 shows the room temperature recorded photoluminescence (PL) spectra of pure chitosan and its ZnO blended samples measured with an excitation of 325 nm. A broad UV emission peak at wavelength of 390 nm was observed for chitosan sample (Kumar, Dutta, & Dutta, 2009). The same peak was noticed as narrow peak in the other three samples (N30, N45 and N60). With these, ultraviolet emission at 422 nm and a strong blue-green emission 495 nm was noticed which may be due to the presence of zinc oxide (Dai, Zhang, & Wang, 2003; Ni et al., 2007).

4. Conclusions

By the addition of zinc chloride during chitosan preparation a novel rod-like chitosan–ZnO complex was formed. Chitosan–ZnO complex formations were confirmed by photoluminescence and FTIR spectroscopy. The particle sizes in nanometer scale and the structure of ZnO were determined by X-ray diffraction analysis. The particle sizes were also evidenced from SEM images. Finally, it is concluded that the variation of NaOH concentration plays a major role for determining the particle size in the complex.

Acknowledgements

The authors would like to thank Alagappa University, Karaikudi, University Grants Commission, New Delhi and Department of Science and Technology, GOI for providing necessary instrumentation facilities and financial support in the form of AURF, SAP and FIST programme respectively.

References

Al-Sagheer, F. A., Al-Sughayer, M. A., Muslim, S., & Elsabee, M. Z. (2009). Extraction and characterization of chitin and chitosan from marine sources in Arabian Gulf. *Carbohydrate Polymers*, *77*, 410–419.

Dai, Y., Zhang, Y., & Wang, Z. L. (2003). The Octa-twin Tetraleg ZnO nanostructures. *Solid State Communication*, *126*, 629–633.

Hong, R., Pan, T. T., Qian, J. H., & Li, H. Z. (2006). Synthesis and surface modification of ZnO nanoparticles. *Chemical Engineering Journal*, *119*, 71–81.

Hubbard, N. B., Culpepper, M. L., & Howell, L. L. (2006). Actuators for micropositioners and nanopositioners. *Applied Mechanics Reviews*, *59*, 324–334.

Kumar, S., Dutta, J., & Dutta, P. K. (2009). Preparation, characterization and optical property of chitosan-phenothiazine derivative by microwave assisted synthesis. *Journal Macromolecular Science. Part A. Pure and Applied Chemistry*, *46*, 1095–1102.

Lee, H. J., Yeo, S. Y., & Jeong, S. H. (2003). Antibacterial effect of nanosized silver colloidal solution on textile fabrics. *Journal of Material Science*, *38*, 2199–2204.

Li, L. H., Deng, J. C., Deng, H. R., Liu, Z. L., & Xin, L. (2010). Synthesis and characterization of chitosan/ZnO nanoparticles composite membranes. *Carbohydrate Research*, *345*, 994–998.

Li, Q., Zhou, J. P., & Zhang, L. N. (2009). Structure and properties of the nanocomposite films of chitosan reinforced with cellulose whiskers. *Journal of Polymer Science. Part B. Polymer Physics*, *47*, 1069–1077.

Muzzarelli, R. A. A. (1973). *Natural chelating polymers*. Oxford: Pergamon Press.

Muzzarelli, R. A. A., & Sipos, L. (1971). Chitosan for the collection from seawater of naturally occurring zinc, cadmium, lead and copper. *Talanta*, *28*, 838–853.

Muzzarelli, R. A. A., & Tubertini, O. (1969). Chitin and chitosan as chromatographic adsorbents and supports for collection of trace metals from aqueous and organic solutions and sea water. *Talanta*, *16*, 1571–1579.

Ni, Y. H., Cao, X. F., Wu, G. G., Hu, G. Z., Yang, Z. S., & Wei, X. W. (2007). Preparation, characterization and property study of zinc oxide nanoparticles via a simple solution-combusting method. *Nanotechnology*, *18*, 1–6.

Qin, C. Q., Xiao, L., Du, Y. M., Shi, X. W., & Chen, J. W. (2002). A new cross-linked quaternized-chitosan resin as the support of borohydride reducing agent. *Reactive and Functional Polymers*, *50*, 165–171.

Son, B., Yeom, B. Y., Song, S. H., Lee, C. S., & Hwang, T. S. (2009). Antibacterial electrospun chitosan/poly(vinyl alcohol) nanofibers containing silver nitrate and titanium dioxide. *Journal of Applied Polymer Science*, *111*, 2892–2899.

Tani, T., Mädler, L., & Pratsinis, S. E. (2002). Homogeneous ZnO nanoparticles by flame spray pyrolysis. *Journal of Nanoparticle Research*, *4*, 337–343.

Tang, E. S. K., Huang, M., & Lim, L. Y. (2003). Ultrasonication of chitosan and chitosan nanoparticles. *International Journal of Pharmaceutics*, *265*, 103–114.

Tang, L. G., & Hon, D. N. S. (2000). Chelation of chitosan derivatives with zinc ions. O,N-carboxymethyl chitosan. *Journal of Applied Polymer Science*, *79*, 1476–1485.

Wang, L., & Muhammed, M. (1999). Synthesis of zinc oxide nanoparticles with controlled morphology. *Journal of Material Chemistry*, *9*, 2871–2878.

Xu, H. Y., Wang, H., Zhang, Y. C., He, W. L., Zhu, M. K., Wang, B., et al. (2004). Hydrothermal synthesis of zinc oxide powders with controllable. *Ceramics International*, *30*, 93–97.

Zhang, X. D., Su, H., Zhao, Y., & Tan, T. (2008). Antimicrobial activities of hydrophilic polyurethane/titanium dioxide complex film under visible light irradiation. *Journal of Photochemistry and Photobiology A: Chemistry*, *199*, 123–129.

Zhu, Y., & Zhou, Y. X. (2008). Preparation of pure ZnO nanoparticles by a simple solid-state reaction method. *Applied Physics A: Materials Science & Processing*, *92*, 275–278.